LANGMUIR

Interface-Rich Materials and Assemblies

2D versus 3D Self-Assembly of a Series of 5-Alkoxyisophthalic Acids

Esther M. Frederick, José David Cojal González, Jürgen P. Rabe, and Steven L. Bernasek

Langmuir, **Just Accepted Manuscript** • DOI: 10.1021/acs.langmuir.8b01827 • Publication Date (Web): 15 Aug 2018

ACS Publications

is published by the American Chemical Society. 1155 Sixteenth Street N.W., Washington, DC 20036

2D versus 3D Self-Assembly of a Series of 5-Alkoxyisophthalic Acids

Esther Frederick[1], José D. Cojal González[2], Jürgen P. Rabe[2] and Steven L. Bernasek*[1,3]

AUTHOR ADDRESS 1 Department of Chemistry, Princeton University, Princeton, NJ 08544, USA

2 Department of Physics & IRIS Adlershof, Humboldt-Universität zu Berlin, D-12489 Berlin, Germany

3 Science Division, Yale-NUS College, 138527 Singapore

KEYWORDS Self-assembly, solvent effects, crystallization, monolayers, scanning tunneling microscopy, x-ray diffraction, hydrogen bonding, van der Waals forces, physisorption.

ABSTRACT: Physisorbed self-assembled monolayers (SAMs) have been suggested as potential models for 3D crystallization. This work studies the effect of altering the chain length of 5-alkoxyisophthalic acid (C_nISA) on self-assembled morphology in both 2D and 3D in order to explore the extent comparisons can be drawn between dimensions. Previous studies of 5-alkoxyisophthalic acid at solid-liquid interfaces (2D) reported different morphologies for C_5ISA and C_6ISA-alkoxy chains on the one hand and C_{10}ISA and C_{18}ISA on the other. Independently, also in 3D a dependence of morphology on chain length has been reported, including an unexpected inclusion of solvent in the 3D morphology of C_6ISA, while the previous reports of 2D self-assembly were driven only by molecule-molecule and molecule-substrate interactions. However, a complete set of data for comparison has been missing. Here we report scanning tunneling microscopy (STM) and molecular dynamics (MD) simulations performed for C_2ISA self-assembled monolayers (SAMs) and STM imaging of C_6ISA−C_9ISA SAMs, to further examine self-assembly behavior in 2D. In 3D, XRD analysis of C_2ISA single crystals was carried out to complete the data set. With a complete set of data, it was observed that regardless of dimension, short chain length C_nISAs formed H-bonding dominated structures, mid-chain length C_nISAs exhibited solvent dependent morphologies, and long chain length CnISAs displayed vdW dominated solvent-independent structures. However, the transition point between morphologies occurred at different chain lengths in 2D and 3D regardless of the dominant interaction. The results of this study inform the design of 2D films and guide the application of knowledge from physisorbed SAMs to 3D systems, including mixed-dimensional (2D/3D) van der Waals heterostructures.

Self-assembly is a process by which unorganized molecules spontaneously organize into self-determined arrangements. In nature, self-assembly plays a key role in the formation of proteins, cells and advanced biological structures. At the nanoscale, self-assembly allows molecules that lack coherence in solution to gain the stability and uniformity needed to operate as functional nanomaterials when adsorbed on a surface.[1] As the lower size limits of top-down architectures of nanostructures are approached, a deeper understanding of how molecules can be programmed to self-assemble into desired architectures becomes increasingly important to the future of nanotechnology.

Surface modification using self-assembled monolayers (SAMs), i.e. well organized single molecule thick layers that spontaneously form at a solid-liquid interface under the appropriate conditions, is a broad and active field of research. Highly complex structures can be designed by careful molecule design.[2,3] In this study, physisorbed SAMs of a series of 5-alkoxyisophthalic acids (C_nISAs) were used to probe the relationship of varying hydrogen bonding (H-bonding) versus van der Waals (vdW) interactions in 2D and 3D self-assembly.

The invention of scanning tunneling microscopy (STM) by Binnig and Rohrer in 1982,[4] enabled an unprecedented level of microscopic imaging at the nanoscale, making it possible to visualize self-assembled structures at solid-liquid interfaces.[5] STM is based on the principle of quantum tunneling, where a tip brought within tunneling distance of the sample is scanned across the surface to provide an electron density map that can be carefully interpreted as surface morphology. The non-destructive nature of STM, makes it the best technique to investigate the morphologies of physisorbed SAMs.

2D self-organized systems have been assumed to be good models for 3D crystallization as the confinement of molecules close to interfaces allows for experimental study of intermolecular forces.[6] Extensive reviews on 2D self-assembly are available covering a range of topics including solvent effects,[7] electronic properties,[8] chirality/odd-even effects,[9] surface-confined supramolecular coordination chemistry,[10] substrate effects,[11] molecular templating,[1] and control of structure.[12] In an attempt to gain better insight into principles guiding formation of physisorbed SAMs, Plass, Grzesiak and Matzger attempted to compile a comprehensive database of all structures as determined by STM studies.[13] The present study explores the validity of the assumed connection between 2D SAM structures and 3D crystals by directly comparing the self-assembly of a series of 5-alkoxyisophthalic acids at the solid-liquid interface with crystallization from solvent in 3D.

Prior investigations of C_nISA crystallization in both 2 and 3 dimensions provided a preliminary, but incomplete set of data for comparison of 2D to 3D morphologies. XRD studies by

Enkelmann, Valiyaveettil, Möessner and Müllen of C_nISA crystal lattices[14] showed that 3D structure is strongly impacted by chain length and solvent effects. Molecules with chain lengths between 6 and 10 carbons formed solvent dependent crystal structures while those with longer chain length incorporate van der Waals interaction to adopt a lamellar architecture. In THF (tetrahydrofuran), a non-hydrogen bonding solvent, molecules with chain lengths between 6 and 10 assembled into H-bonded hexamer channels with alkyl chain walls. However, when methanol (MeOH) was used as a solvent, the MeOH co-adsorbed with the C_nISA head groups to form VdW ribbons with ordered alkyl chains. Longer C_nISAs assembled into ribbons via C_nISA chain-chain interactions and did not co-adsorb with either solvent. Solvent and chain length effects were also observed for the self-assembled 3D structures of 5-alkoxyisophthalic acids with first row transitions metals.[15]

Studies by Dickerson *et al.* of C_nISA SAMs[16] demonstrated a similar phenomenon at the solid-liquid interface, where shorter chain length SAMs formed a solely hydrogen bonded network morphology (C_6 and below) while longer chain length SAMs (C_{10} and up) formed a lamellar structure with hydrogen bonding between head groups and VdW interaction between chains. This prior study did not experimentally explore the morphology of SAMs with chain lengths 6−10 to determine the chain length of the transition point. Studying the transition between SAM morphologies is a critical component for understanding the thermodynamics of self-assembly.[17] The current study determined the exact chain length of the transition point from hexagonal to lamellar morphology to help determine how molecular interactions affect the architecture, as well as obtain a more complete picture of the relationship between the 2D and 3D self-assembly.

The comparison of self-assembly in multiple phases has literary precedence. A study of C_{16}ISA compared the self-assembly of C_nISA both in the crystal lattice and at a highly oriented pyrolytic graphite (HOPG) interface.[18] In both the 2D and the 3D structures, the pure C_{16}ISA formed lamellar structures of packed interdigitating acids. The H-Bonding structures differed due to larger degrees of freedom in 3D, which allowed the H-bonding heads and alkyl chains to pack in separate planes. In 2D, by contrast, the two are confined to the same plane. C_{16}ISA and C_{12}ISA were further explored in both dimensions co-adsorbed with pyrazine and 2.5-dimethylpyrazine.[19] Additionally, when developing the Two-Dimensional Structural Database (2DSD), which compiles physisorbed SAM structures characterized using STM, Plass et. al.[13] noted similarities between the factors governing 2D and bulk structures though the actual packing differed. Other studies have focused on molecules such as polymers,[20] organometallic complexes[21], discotic liquid crystals[22] and biological materials, such as guanosine,[23] to compare the structures in 2D and 3D, however to the best of our knowledge systematic studies, comparing the effects of varying the chain length of a substituent on morphology in 2D versus 3D have not been done. Continued contributions to the 2DSD with systematic experimental and theoretical studies are essential for the development of predictive models for 2D self-assembly.[13,24]

This work presents a systematic study comparing multi-phase assembly of C_nISA with a series of alkoxy chain lengths to analyze the extent 2D SAMs can act as models for 3D systems, specifically testing for similarity in morphology and whether the chain length of the transition point remains the same in 2D as in 3D. While some of the data is present in the literature, further experiments were needed to complete the data set required to examine the effect of dimension on self-assembly. The available literature data and experimental list for this study are organized in Table 1.

Table 1: Literature data (in black) and experiments unique to this study (in red) for multi-phase 5-alkoxyisophthalic acid self-assembly.

C_nISA molecule	2D results	3D results
Short Chain	C_2ISA	C_2ISA
Mid Chain	C_5ISA, C_6ISA:[16] H-bonded network C_7ISA, C_8ISA, C_9ISA	Solvent-dependent structures:[14] H-bonded network in THF, H-bond guided lamellar in MeOH
Long Chain Lengths	C_{10}ISA, C_{18}ISA:[16] vdW dominated lamella	$C_{12\text{-longer}}$ISA:[14] vdW dominated lamella

In the present study, the crystal structure of C_2ISA has been obtained and the morphology of a series of C_2ISA, C_6ISA−C_9ISA SAMs has been determined to supplement literature results from XRD studies of 5-alkoxyisophthalic acid crystals[14] and STM studies of C_nISA SAMs.[16] A complete comparison of short chain length (C_2ISA), mid chain length (C_6ISA−C_{10}ISA), and long chain length (C_{18}ISA) ISAs is provided.

EXPERIMENTAL

Synthesis: C_nISAs were synthesized according to the schematic below (Figure 1). Sn2 substitution with the appropriate iodoalkane was used to convert dimethyl 5-hydroxyisophthalate to dimethyl 5-alkoxyisophthalate. 6 mmol of the respective alkyl iodide (ThermoFisher Scientific, 98%) and 6 mmol of K_2CO_3 dissolved in 7.5 mL acetone were placed in a three neck round bottom flask under an argon environment. 1.05 g of dimethyl 5-hydroxyisophthalate (Sigma-Aldrich, Germany, 98%) was dissolved in 7.5 mL acetone and added via syringe to the flask. Reactants were refluxed at 75° for 24−48 hours. To monitor the reaction progress, aliquots were removed, rotovapped and analyzed with mass spectroscopy. When the reaction was complete, the product was rotovapped and purified by silica flash column chromatography using a 10:90−20:80 acetone/hexanes eluent. To form C_nISA, the product was further reacted with KOH. The reaction was monitored as previously with mass spectroscopy. The resulting C_nISA was purified by separatory funnel extraction. The C_nISA was dissolved in 10 mL water, acidified using 1 M HCl and then extracted into diethyl ether. The product was dried using Na_2SO_4 for 2 hours, then rotovapped to remove remaining solvent and placed on high vacuum overnight. Resulting fine white powder was analyzed with ^{1}H NMR and ^{13}C NMR (Bruker 500 AVANCE spectrometer) as

presented in the supplemental information (See SI 1). Recrystallization of C_2ISA for XRD studies was done according to literature procedures using THF.[14]

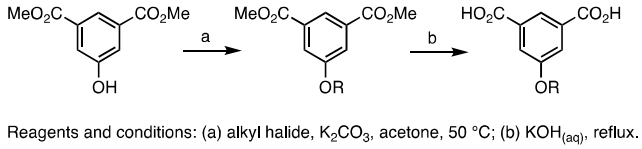

Figure 1: Synthetic scheme for 5-alkoxyisophthalic acid.

STM Imaging: Obtaining an ordered structure at the solid-liquid interface can be a difficult endeavor requiring skill and experience. Ordered monolayers formed from molecules with a strong preference for ordering such as the C_9ISA were more easily obtainable relative to others, such as the C_2ISA, which required many attempts. In brief, several ~1 mM solutions of the desired C_nISA in phenyloctane (Aldrich, 98%) were prepared using sequential dilutions sonicated at 60°C for 1 hour. Monolayer formation was attempted for each slightly varying concentration by placing a few drops of the respective solution onto freshly cleaved HOPG (NanoScience Instruments, Research Grade). Samples were placed in the freezer for 1 hour to allow for monolayer formation. Freezing was not necessary for monolayer formation, but produced clearer images than assemblies formed at room-temperature. After removing from the freezer, samples sat at room temperature for at least one hour to equilibrate to ambient conditions before imaging. Images were obtained with freshly cut Pt/Ir tips (NanoScience Instruments, 80/20,0.25mm diameter). Reproducible images from several different samples were obtained for each C_nISA.

For all except C_2ISA, images were obtained using an ambient Nanosurf AG EasyScan STM system (NanoScience Instruments, Liestal, Switzerland) in constant current mode with various tunneling conditions (V_b = 0.4−0.8 V, I_t = 0.7−0.9 nA). As this instrument places bias on the tip rather than the sample, a positive bias was used so electrons tunneled from the sample to the tip. In the case of C_2ISA, a home-built ambient STM with an Omicron controller was used to obtain images, with a negative bias voltage placed on the sample (V_S) to ensure electrons tunneled from sample to tip. Height and current measurements were collected for all scans. Post imaging analyses were done using SPIP (Image Metrology A/S). Fourier Transform (FT) analyses of the current scan were used to calibrate images with underlying HOPG. FT analyses of the corrected height image were used to determine SAM unit cell parameters. Long range scans and C_8ISA images were not calibrated as the underlying HOPG was not well-enough resolved in these images to provide a meaningful calibration. Proposed structures were modeled with Avogadro.[25,26] Monolayer formation was confirmed by measuring line profiles over the edge of the ordered domain onto the bare HOPG surface.

XRD: Crystals were formed by placing saturated THF solutions of the desired C_nISA in the freezer for several weeks. Structures were obtained using Bruker D8 Venture and analyzed using the SQUEEZE method in the program PLATON which compensated[27] for the scattering from the disordered solvent. Images of the structures were created using Vesta.[28]

MD: Molecular dynamics simulations were performed using NAMD[29] (2.10 build for Linux) with CHARMM general force field (CGenff).[30] A Langevin thermostat with a 1 ps^{-1} damping coefficient and a 2 fs time step was used in all simulations. A distance cutoff of the size of the periodic box was used to compute non-bonded interactions. Electrostatic interactions were calculated using the Particle mesh Ewald (PME) method with a space grid of 0.5 Å. As in previous work, a graphene slab was constructed as a substrate to simulate molecular adsorption on HOPG.[31] In all simulations, the substrate was fixed and its atoms were assigned atom type CG2R61 with no partial charge. Parameters for the C2ISA molecule were assigned by CGenff analogy. 20 ns MD simulations were performed for different combinations of molecules per cluster, including both C_2ISA and 1-phenyloctane. A snapshot of the simulation was taken every 20 ps and rendered according to the contribution of each atom to the tunneling current.[32] STM simulated MD trajectory images were calculated by averaging a minimum of 1000 frames.

RESULTS

STM Results: C_2ISA: C_2ISA formed SAMs with bright areas arranged in a highly hexagonal pattern (Figure 2) with long range order (Figure SI 2.1). The average unit cell, incorporating both dark and bright areas (as depicted in Figure 2a), was measured as a= 2.22 ± 0.17 nm, b= 2.14 ± 0.24 nm, $\angle_{a,b}$ = 61 ± 3°. The bright spots, corresponding to regions of higher electron density due to adsorbed molecules, did not reveal highly resolved molecules. Computational methods (described in SI 2 and SI 3) were undertaken to gain insight into the unit cells. A statistical particle analysis (Figure SI 2.2) measured an average size of 1.5 ± 0.1 nm for the regions of higher electron density, which is 50% more than the maximum length of C_2ISA (~1 nm). Due to this, each bright spot was assumed to be a cluster of several molecules, either C_2ISA or a co-adsorption of C_2ISA with 1-phenyloctane.

Trimer-solvent clusters were identified as the best candidates for initial MD simulations (Figure 2b). DFT calculations at the B3LYP/6-31g(d,p) level showed trimer formation lead to a gain of 105 kJ/mol, which equals 35 kJ/mol per molecule. This result is in good agreement with the published value of 60−66 kJ/mol, obtained by measuring the enthalpy of hydrogen bonding in carboxylic acid dimers.[33] Structures formed by less than three molecules were not large enough to fit the measured STM data. Clusters of four molecules were energetically less favorable (~25 kcal/mol per unit cell from MD simulation analysis) than three molecule clusters. Preliminary models for clusters of five and six molecules displayed close-packing which constrained the molecules to the initial conformation, and therefore were not further considered.

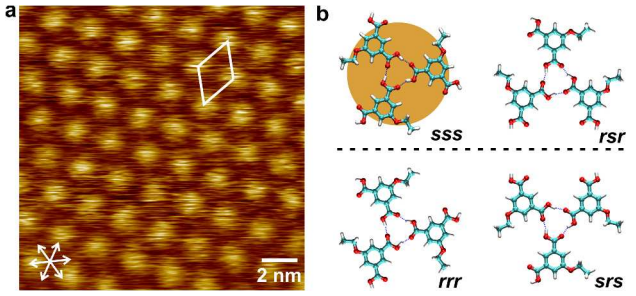

Figure 2: (a) 20 × 20 nm STM height image of C_2ISA in 1-phenyloctane assembled on HOPG. White arrows show the orientation of the graphite underneath (V_S = -0.30 V, I_t = 0.40 nA). **(b)** C_2ISA can arrange in 4 different in-plane trimers. The orange circle represents the average size of the bright spots

A tunneling current simulation method, previously shown to accurately reproduce STM images of soft supramolecular networks,[32] was used to account for transitory non-trimer intermediate structures formed during the simulation. For the starting configuration, four trimers and eight solvent molecules (filling the gaps in between trimers) were placed in a hexagonal box with periodic boundary conditions to reproduce an infinite system. The hexagonal box was developed using the unit cell parameters of Figure 2a, leading to a periodic box of four unit cells as displayed in Figure 3b. The xyz positions of all components were recorded every 20 ps in snapshot files, with every simulation running for 20 ns. The MD tunneling current simulation (Figure 3b) was then produced by averaging the 1000 snapshot files collected throughout the simulation. Eight different 20 ns MD simulations were performed to take into account all possible chirality combinations four C_2ISAs can form when adsorbed parallel to the substrate (Figure 2b). The resulting images were then averaged to produce a MD simulation (Figure 3a) representative of all possible trimer chirality combinations. The average of these MD simulations was the closest fit to experimental STM image, with a simulated unit cell of $a = 2.21 \pm 0.10$ nm, $b = 2.21 \pm 0.10$ nm, $\angle_{a,b} = 59 \pm 1°$. This result suggests that the hexagonal experimental pattern is due to conformational freedom in the arrangement of energetically favorable and hydrogen-bond driven trimers. See SI 3 for a more detailed breakdown of the MD simulations.

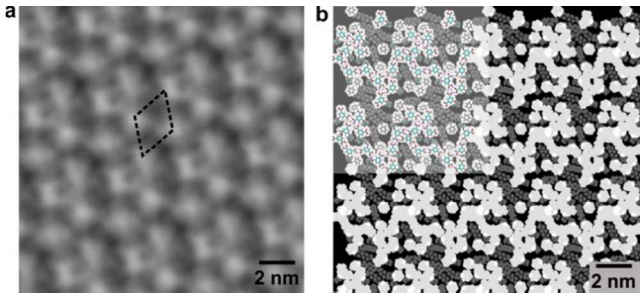

Figure 3: (a) 20 × 20 nm simulated STM measurement calculated by averaging the MD trajectories of the 8 potential trimer combinations. **(b)** Render of the tunneling current for a 5×5 periodic simulation box (10 × 10 unit cells) after 20 ns of MD simulation at 300K. One periodic box (2 × 2 unit cells) is greyed with the molecular structure imposed. The hydrogen bonds in the models go beyond the periodic box.

<u>C_7ISA – C_9ISA:</u> Long range ordered lamellar SAMs were observed for C_7ISA−C_9ISA SAMs (Figure 4 and Figure 5b).

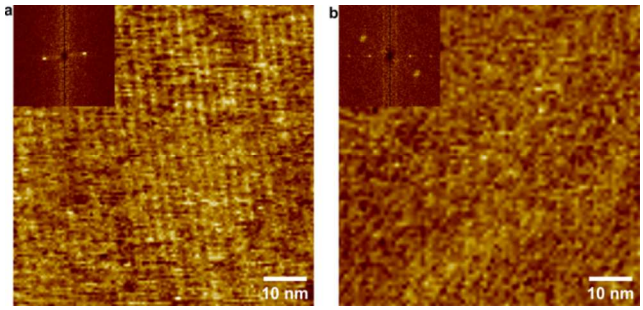

Figure 4: ~60 x 60 nm STM height images of (a) C_7ISA (V_b = 0.48V, I_t = 1.0 nA) and (b) C_8ISA (V_b = 0.70V, I_t = 0.77 nA) displayed long range ordered SAMs, further demonstrated in the inset FFT.

C_9ISA images had the best resolution and will be used to describe the SAM formation results at these chain lengths. C_9ISA formed highly ordered SAMs with lamellar patterns of alternating dark and light stripes. As mentioned in the experimental section, light stripes were attributed to regions of greater electron density, and as such represent the aromatic head groups which have greater electron density as compared to alkyl chains, while dark stripes were attributed to the alkyl chains. After calibration to HOPG, the FFT of the height image displayed two sets of bright spots which shared one common spot (red) representing two related parallelogram cell structures (see Figure 5). In both unit cells; a = the shorter side running along the bright stripe, b = the side spanning the distance between the bright lines and $\angle_{a,b}$ = the angle between the two sides. The cyan-red set corresponded to the larger unit cell spanning the distance between stripes, with unit cell values of $a = 0.6 \pm 0.3$ nm, $b = 3.3 \pm 0.3$ nm, $\angle_{a,b} = 83 \pm 4°$. The green-red set corresponded to the unit cell spanning halfway between with a change to the b parameter only, with $b = 1.3 \pm 0.3$ nm. The large error in the a parameter value demonstrates that the spacing along the bright stripes cannot be confidently assigned. The resolution of the images only allows for establishing the b parameter value.

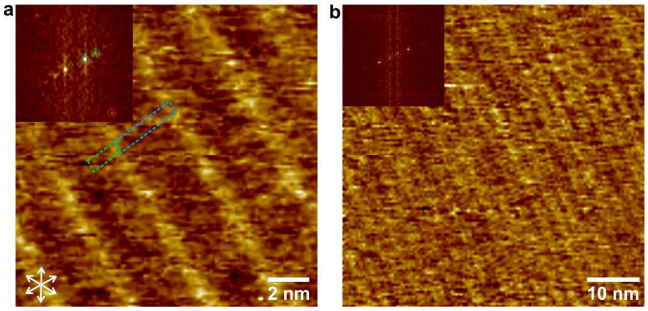

Figure 5: C_9ISA unit cell and FFT. **(a)** 15 x 15 nm C_9ISA height image after calibration to HOPG with inset FFT. The FFT displayed two sets of bright spots, which shared one common spot (red) (V_b = 0.76 V, I_t = 0.77 nA)**.** The white arrows indicate symmetry directions of the underlying HOPG. **(b)** ~60 x 60 nm STM height image of C_9ISA. The 2D hexagonal network displayed long range order, further demonstrated in the inset FFT (V_b = 0.66 V, I_t = 0.80 nA).

The first suggested structure involved interdigitated adjacent C_9ISA molecules with an H-bonded backbone as in previous work. This model yielded lamellae of 2.1 nm, which was 1.3 nm too small to fit the measurements. The proposed model that best fit this data consisted of a unit cell containing two C_9ISA groups laid tail to tail without alkyl chain interdigitation and H-bonding between adjacent head groups (see Figure 6). As this model was energetically unfavorable, incorporation of phenyloctane solvent molecules was proposed as a stabilizing factor. The exact orientation of the molecules could not be determined. As the head groups were typically not visible, it is most likely that the alkyl chains are lying flat on the substrate with the head groups tilted upward from the surface. Moreover, one of the symmetry axes of the underlying HOPG is oriented about 5° with respect to the vector ***b***. This suggests that the alkyl chains lie along this symmetry axis, which would also maximize the vdW interactions between the alkyl chains and the substrate. The smaller structure could then be explained as the repeating unit of a single phe-

nyloctane and C_9ISA molecule. The larger structure, containing two C_9ISA molecules, was taken as the unit cell as its replication produced a schematic that lined up well with experimental measurements.

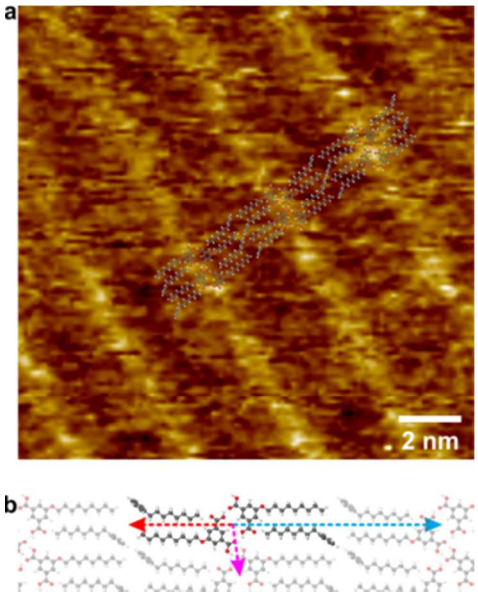

Figure 6: 15 x 15 nm C_9ISA STM image with **(a)** overlaid proposed structural model and **(b)** structural model (V_b = 0.76 V, I_t = 0.76 nA). The arrows on the model correspond to the circled spots in the FFT in Figure 5. The underlying HOPG lattice is indicated in Figure 5a.

C_7ISA and C_8ISA also displayed lamellar SAMs. The distance between the bright lines in the C_7ISA was measured as 3.0 ± 0.6 nm (Figure 7). These values were too large to fit the intermolecular alkyl chain interdigitation model of 1.7 nm. Also of note, in the C_7ISA, several bright spots appeared halfway between the lamellae (see Figure 7 and SI 4). These spots could potentially be attributed to disorder of the incorporated solvent molecules leading to random head groups serendipitously oriented in a manner that could be imaged. C_8ISA images were not of high enough resolution to confidently calibrate to the underlying HOPG. Both the uncalibrated image and attempted calibrations led to b-values of 3.1 ± 0.9 nm. The lower end of the error 2.2 nm value is still higher than the expected 1.9 nm. As the C_8ISA falls between two solvent incorporated lamellae, it is most likely that the C_8ISA SAM also involves phenyloctane incorporation.

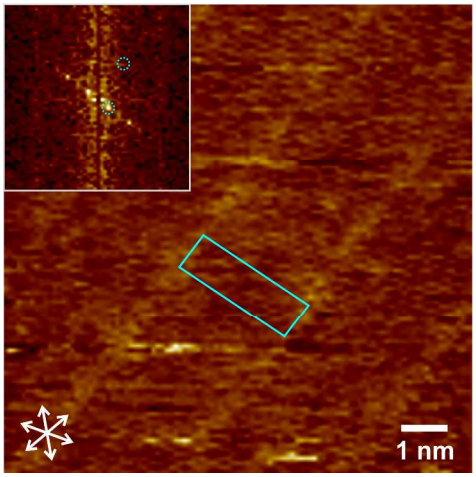

Figure 7: 10 nm x 10-nm C_7ISA height image with unit cell (V_b = 0.72 V, I_t = 0.70 nA). The white arrows indicate the orientation of the underlying HOPG.

C_{10}ISA: Due to the surprising solvent incorporation in C_6ISA−C_9ISA SAMs, C_{10}ISA images from previously published work were re-examined. A re-analysis demonstrated *b*-values of 2.6 ± 0.3 nm nm which matches the alkoxy-alkoxy C_{10}ISA chain interdigitation model proposed previously by Dickerson *et al.*[16] Therefore, the transition point between solvent dependent and solvent-independent morphologies was found to be C_{10}ISA.

The hypothesis that a transition point would be found was substantiated. However, the transition point was significantly more complex than what might be expected based on intermolecular C_nISA interactions and substrate-molecule interactions alone. The unexpected incorporation of solvent at the transition point leads to a whole new set of questions to be explored in future work. What is the dependence of this transition point on the solvent? Can the transition point be pushed to higher and lower chain lengths by changing the chain length of the solvent? While solvent dependence on physisorbed SAM morphology has been previously explored,[6,34-39] the ability to achieve solvent-independent SAM morphologies by altering the chain-length of a moiety on an integral SAM component is an interesting discovery.

XRD Results: XRD structure determinations showed C_2ISA formed $P2_{1/c}$ space group crystals with unit cell parameters of a = 12.02 Å b = 12.46 Å c = 16.76 Å and angles α = γ = 90° and β = 107.77° (see SI for CIF file). Crystal structure views along the *a* and *c* axes displayed four sheets of molecules layered one upon another without chemical connection (Figure 8). The view along the *c*-axis showed benzene ring alignment for the middle two molecules, strongly suggesting the layers were held together by π−π stacking forces. As previously observed in Enkelmann's[14,40] work, these structures were dominated by H-bonding and consisted of stacked layers of tape-like sheets. The current studies provide unit cell measurements and a detailed analysis not seen in previous work.

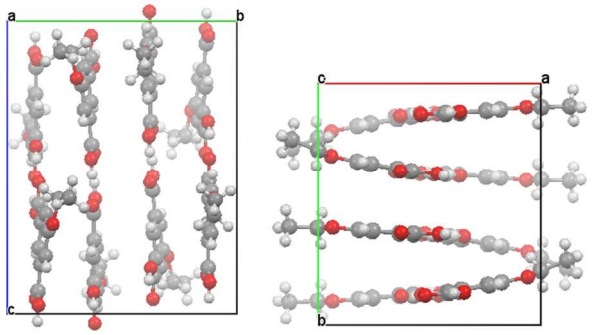

Figure 8: 3D crystal structure of C_2ISA viewed along the *a* axis (left) and c-axis (right).

The view along the *b*-axis (Figure 9) showed that each layer consisted of two molecules per each unit cell. Within the layer, molecules formed carboxylic acid dimers held together by hydrogen bonding intermolecular interactions between head groups. Adjacent dimers were further H-bonded to neighboring dimers on both sides to form ribbons. The ribbons were not connected to each other, which agreed with previous results.

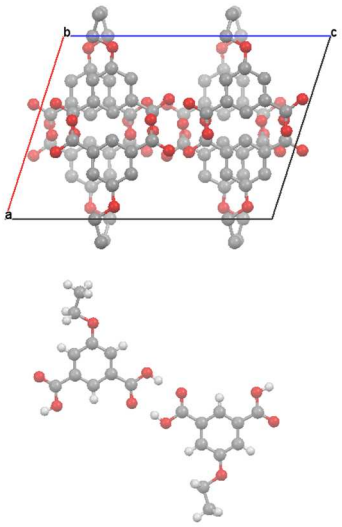

Figure 9: 3D crystal structure of C_2ISA viewed along the b-axis. *Top*: b-axis view of the full four-layered unit cell with hydrogens omitted for clarity. *Bottom*: A single layer.

DISCUSSION

To summarize, while details of the structures were dimensionality dependent, at a given chain length, there was a strong similarity for the trends in forces that governed self-assembly of C_nISA regardless of dimension (see Table 2).

At chain lengths below C_7ISA in SAMs and below C_7 ISA in 3D, assembly was driven by intermolecular H-bonding interactions without VdW contributions. Published values for van der Waals chain-chain interactions are 6−7 kJ/mol per carbon[16,41] and enthalpy of hydrogen bonding in carboxylic dimers determined from dimer dissociation energies are 60−66 kJ/mol.[33] In SAMs, the observed morphology involved C_nISA molecules with 60−66 kJ/mol H-bonding intermolecular interactions plus unquantified substrate, solvent and entropy values and no involvement of chain-chain vdW interactions, which would contribute 36−42 kJ/mol.

At mid-chain lengths between C_7ISA−C_9ISA in SAMs and C_6ISA−C_{12}ISA in 3D, solvent dependent morphologies were observed. The surprising inclusion of solvent in SAMs of C_7−C_9ISA indicates the formation of mid-chain length SAMs is more complex than had been expected based on previous C_nISA SAM work.[16] The observation can be explained by the following: SAM formation occurs when the gain in enthalpy due to intermolecular and surface-molecule interactions overcomes the otherwise unfavorable ordering. There are similar enthalpy gains for a neat or mixed C_nISA/phenyloctane SAMs for C_7ISA−C_9ISA with a maximum difference of one vdW interaction per molecule. The decrease in entropy that must be overcome for SAM formation is less for a mixed monolayer SAM which incorporates multiple species and therefore has more variety than a neat SAM. It is also important to note that mixed SAMs formed at chain lengths (n = 7−9) that matched closely to the solvent chain length of 8 carbons. Therefore, the mixed monolayer formation for C_7ISA and C_9ISA is attributed to the lower entropic cost of formation combined with similar enthalpy gains and optimal packing as in the neat SAMs. As no neat SAMs were observed, it is likely that the enthalpy gains are not high enough to overcome the entropic cost of forming a neat monolayer.

Above C_{10}ISAs, both 2D and 3D assemblies exhibited lamellar morphologies without solvent inclusion. At these chain lengths, the forces governing the assembly are similar. However as previously noted by Enkelmann *et al.*,[14] the details of the H-bonding arrangements are dimension dependent. As before, the SAM morphology can be explained by the balance between entropic cost of ordering and enthalpy gains from intermolecular and surface interactions. The unfavorable ordering of a neat monolayer is overcome by the increased vdW interactions at chain lengths of 10 carbons and above. The energetic difference between whether C_nISA form a neat and mixed SAM in phenyloctane on HOPG is on the order of 3 additional vdW interactions (C_{10}ISA−C_{10}ISA versus C_7ISA−C_7ISA), which is at most 49 kJ/mol.

The goal of finding a quantitative transition point between differing morphologies was achieved. However, the unexpected inclusion of the solvent at the transition point meant this transition point was more complicated than the expected C_nISA−C_nISA interactions. Two transition points were observed. The first was the transition from a H-bonded C_6ISA SAM to a solvent-dependent lamellar C_7ISA SAM, while the second was the transition from a solvent-dependent lamellar C_{10}ISA SAM to a solvent-independent C_{11}ISA SAM.

Interestingly, the transitions between morphologies occurred at different chain lengths in 2D SAMs than in 3D crystals. It is important to emphasize that the experimental conditions for 2D SAMs used phenyloctane as a solvent, while the literature and experiment results for 3D crystals used MeOH and/or THF. Therefore, it is not yet known if the difference in the chain length of morphology transition is due to substrate effects or due to solvent interactions. Experiments with the same solvent at these chain lengths would be of use for further quantifying these relationships and determining the extent to which the substrate stabilized the interactions. Additionally, flow micro calorimetry experiments and molecular mechanics

simulations to quantify the enthalpy of adsorption as done by Barnard and Matzger[42] would be useful to further understand the behavior of the system.

It is of great interest to further this work in collaboration with theorists. Devising a model from this experimental data that can be used to predict future structures could provide insight into generalizable rules for self-assembly. While a generalizable model for surface assembly has thus far not been possible, the study of complex systems such as those in this work provide the detailed information necessary for insight into the patterns of self-assembly across different systems. A deep understanding of similarities in self-assembly behavior is necessary for developing a generalizable theoretical framework.

Table 2: Summary of literature and experimental structure results for multiphase C_nISA self-assembly

C_nISA molecule	2D results	3D results
Short Chain Lengths	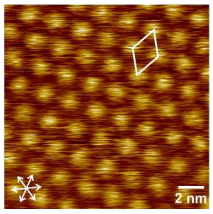	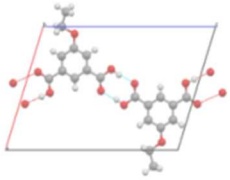
	H-Bonding governed structures	
Mid Chain Lengths	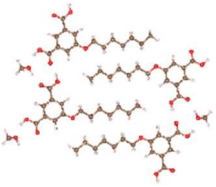	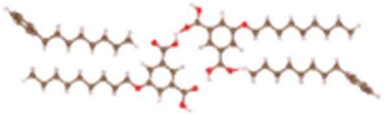
	Solvent dependent structures	
Long Chain Lengths	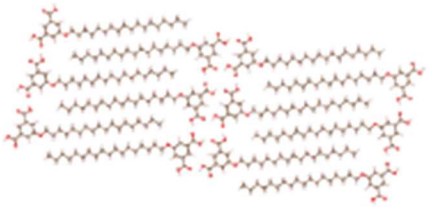	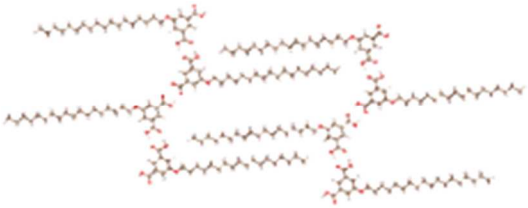
	vdW dominated structures, no solvent effects	

CONCLUSIONS

In conclusion, 5-alkoxyisopthalic acids were used as model systems for comparing 2D and 3D self-assembly. Similar trends were observed for the forces governing self-assembly, however the chain lengths of morphological transitions and the finer details of the assemblies differed. This work demonstrates that 2D systems may be used to inform the behavior of forces in 3D self-assembly, however care must be taken when working in transition regions.

Shorter chain C_nISA molecules exhibited H-bonding morphologies in both phases, with network structures for C_2ISA−C_6ISA SAMs and dimer tape structures for C_2ISA−C_5ISA 3D crystals. The mid-chain length molecules, C_6ISA−C_9ISA SAMs and C_7−C_{12}ISA 3D crystals exhibited solvent dependent morphologies, with SAMs forming wide lamella with unexpected phenyloctane-C_nISAs alkyl chain interdigitation and 3D structures forming layered ring or lamellar structures in THF and MeOH respectively.[14] The long chain structures, starting at C_{10}ISA in 2D and at C_{13} in 3D, exhibited solvent independent lamellar morphologies.

Interestingly, the transitions between morphologies occurred at different chain lengths in 2D SAMs than in 3D crystals. Further experiments using the same solvent in both dimensions and exploring other substrates would be of interest to further elucidate the substrate contribution to SAM stability. The unexpected solvent dependent morphologies observed for mid-chain length 2D SAMs leads to an interest in exploring whether solvent-independent film morphologies are attainable by altering the chain-length of a moiety on an integral SAM component. This work adds to the continual exploration of physisorbed SAMs, which is crucial to building the data needed to develop models for predicting SAM and thin film morphology, including mixed-dimensional (2D/3D) van der Waals heterostructures.[43]

ASSOCIATED CONTENT

Supporting Information. C_nISAs NMR data, C_2ISA MD simulation information, C_2ISA CIF file. This material is available free of charge via the Internet at http://pubs.acs.org.

AUTHOR INFORMATION

Corresponding Author

*sberna@princeton.edu

Author Contributions

The manuscript was written through contributions of all authors. All authors have given approval to the final version of the manuscript.

ACKNOWLEDGMENT

This work was partially supported by the National Science Foundation, Division of Chemistry, CHE-1213216, the Division of Materials Research, DMR-1506989 and the Deutsche Forschungsgemeinschaft, SFB-765. ETF acknowledges the support of Humboldt-talent travel grant within the Princeton-Humboldt University Profile Partnership, NSF-GRFP for funding and Professor Jeffrey Schwartz and Travis Shaw for useful discussions, and Erin Grey for ChemDraw edits. We acknowledge Phil Jeffrey, PhD, for XRD structures.

ABBREVIATIONS

C_nISA, 5-alkoxyisophthalic acids; SAM, self-assembled monolayer; H-bonding, hydrogen bonding; vdW, van der Waals; STM, scanning tunneling microscopy; HOPG, highly oriented pyrolytic graphite.

REFERENCES

1. Shan-Shan, L.; Northrop, B. H.; Yuan, Q.; Wan, L. J.; Stang, P. J. Surface Confined Metallosupramolecular Architectures: Formation and Scanning Tunneling Microscopy Characterization. *Acc. Chem. Res.* **2009**, 249.
2. Ahn, S.; Matzger, A. J. Six Different Assemblies from One Building Block: Two-Dimensional Crystallization of an Amide Amphiphile. *J. Am. Chem. Soc.* **2010**, *132*, 11364-11371.
3. Xue, Y.; Zimmt, M. B. Patterned Monolayer Self-Assembly Programmed by Side Chain Shape: Four-Component Gratings. *J. Am. Chem. Soc.* **2012**, *134*, 4513-4516.
4. Binnig, G.; Rohrer, H. Scanning Tunneling Microscopy - From Birth to Adolescence. *Rev. Mod. Phys.* **1987**, *59*, 615-625.
5. (a) Mizutani, W.; Shigeno, M.; Ono, M.; Kajimura, K. Voltage-Dependent Scanning Tunneling Microscopy Images of Liquid Crystals on Graphite. *Appl. Phys. Lett.* **1990**, *56*, 1974-1976. (b) Rabe, J.P.; Buchholz, S. Commensurability and Mobility in Two-Dimensional Molecular Patterns on Graphite. *Science*, **1991**, *253* (5018), 424-427. (c) Rabe, J.P.; Buchholz, S. Direct Observation of Molecular Structure and Dynamics at the Interface Between a Solid Wall and an Organic Solution by Scanning Tunneling Microscopy. *Phys. Rev. Lett.* **1991**, *66*(16), 2096-2099.
6. Liu, P.; Miao, X.; Li, Z.; Zha, B.; Deng, W. Two-dimensional Self-assembly of Single-, Poly- and Co-crystals at the Liquid/Solid Interface. *Cryst. Eng. Comm.* **2014**, *41*, 9690 - 9696.
7. (a) Elemans, J. A. A. W.; De Feyter, S. Structure and Function Revealed with Submolecular Resolution at the Liquid-Solid Interface. *Soft Matter* **2009**, 721-735. (b) Yang, Y.; Wang, C. Solvent Effects on Two-Dimensional Molecular Self-Assemblies Investigated by Using Scanning Tunneling Microscopy. *Curr.Opin. Colloid Interface Sci.* **2009**, 14, 135 - 147.
8. Amabilino, D. B.; De Feyter, S.; Lazzaroni, R.; Gomar-Nadal, E.; Veciana, J.; Rovira, C.; Abdel-Mottaleb, M. M.; Mamdouh, W.; Iavicoli, P.; Psychogyiopoulou, K.; Linares, M.; Minoia, A.; Xu, H.; and Puigmart, J. Monolayer Self-Assembly at Liquid-Solid Interfaces: Chirality and Electronic Properties of Molecules at Surfaces. *J. Phys. Condens. Matter* **2008**, *20*, 184003.
9. (a) Tao, F.; Bernasek, S. L. Understanding Odd-Even Effects in Organic Self-Assembled Monolayers. *Chem. Rev.* **2007**, *107*, 1408-1453. (b) De Feyter, S.; De Schryver, F. C. Self-Assembly at the Liquid/Solid Interface: STM Reveals. *J. Phys. Chem. B* **2005**, *109*, 4290-4302.
10. (a) Lin, N.; Stepanow, S.; Ruben, M.; Barth, J. Surface-Confined Supramolecular Coordination Chemistry. In *Templates in Chemistry III*; Broekmann, P., Dötz, K. and Schalley, C., Eds.; Springer Berlin / Heidelberg: 2009; Vol. 287, pp 1-44.
11. Barth, J. V. Molecular Architectonic on Metal Surfaces. *Annu. Rev. Phys. Chem.* , 375.
12. De Feyter, S.; De Schryver, F.C. Two-Dimensional Supramolecular Self-Assembly Probed by Scanning Tunneling Microscopy. *Chem. Soc. Rev.* **2003**, *32*, 139-150.
13. Plass, K. E.; Grzesiak, A. L.; Matzger, A. J. Molecular Packing and Symmetry of Two-Dimensional Crystals. *Acc. Chem. Res* **2007**, *40*, 287-293.
14. Enkelmann, V.; Valiyaveettil, S.; Möessner, G.; Müllen, K. Self-Assembly of 5-Alkoxyisophthalic Acids: Alkyl Chain Length Dependence for the Formation of Channel-Type and Sheet-Type Structures. *Supramol. Sci.* **1995**, *2*, 3-7.
15. McCormick, L.J.; Morris, S.A.; Slawin, A.M.Z.; Teat, S.J.; Morris, R.E. Coordination Polymers of 5-Alkoxy Isophthalic Acids. *Cryst. Growth Des.*, **2016**, *16* (10), 5771–5780.
16. Dickerson, P. N.; Hibbard, A. M.; Oncel, N.; Bernasek, S. L. Hydrogen-Bonding versus van der Waals Interactions in Self-Assembled Monolayers of Substituted Isophthalic Acids. *Langmuir* **2010**, 18155.
17. Blunt, M. O.; Adisoejoso, J.; Tahara, K.; Katayama, K.; Van, d. A.; Tobe, Y.; De Feyter, S. Temperature-Induced Structural Phase Transitions in a Two-Dimensional Self-Assembled Network. *J. Am. Chem. Soc.* **2013**, *135*, 12068-12075.
18. Valiyaveettil, S.; Mullen, K. Multiphase Self-Assembly of 5-Alkoxyisophthalic Acid and its Applications. *New J. Chem.* **1998**, *22*, 89-95.
19. Eichhorst-Gerner, K.; Stabel, A.; Moessner, G.; Declerq, D.; Valiyaveettil, S.; Enkelmann, V.; Müllen, K.; Rabe, J. P. Self-Assembly of a Two-Component Hydrogen-Bonded Network: Comparison of the Two-Dimensional Structure Observed by Scanning Tunneling Microscopy and the Three-Dimensional Crystal Lattice. *Angewandte Chemie International Edition in English* **1996**, *35*, 1492-1495.
20. Samorí, P.; Francke, V.; Enkelmann, V.; Müllen, K.; Rabe, J. P. Synthesis and Solid State Structures of Functionalized Phenyleneethynylene Trimers in 2D and 3D. - *Chem. Mater.* **2003**, *15*, 1032 - 1039.

21. Tong, M.; Zheng, S.; Chen, X. Self-Assembly of Two- and Three-Dimensional Coordination Networks with Hexamethylenetetramine and Different Silver(I) Salts. *Chemistry – A European Journal* **2000**, *6*, 3729-3738.
22. Ruan, P.; Xiao, B.; Ni, H. L.; Hu, P.; Wang, B. Q.; Zhao, K. Q.; Zeng, Q. D.; Wang, C. The Influence of Alkyl Chain Substitution Pattern on the Two- and Three-Dimensional Self-Assembly of Truxenone Discogens. *Liquid Crystals* **2014**, *41:8*, 1152 - 1161.
23. Gottarelli, G.; Masiero, S.; Mezzina, E.; Pieraccini, S.; Rabe, J. P.; Samorí, P.; Spada, G. P. The Self-Assembly of Lipophilic Guanosine Derivatives in Solution and on Solid Surfaces. *Chemistry – A European Journal* **2000**, *6*, 3242-3248.
24. Palma, C.; Cecchini, M.; Samori, P. Predicting Self-Assembly: From Empirism to Determinism. . *Chem. Soc. Rev.* **2012**, *41*, 3713 - 3730.
25. Hanwell, M. D.; Curtis, D. E.; Lonie, D. C.; Vandermeersch, T.; Zurek, E.; Hutchinson, G. R. Avogadro: An Advanced Semantic Chemical Editor, Visualization, and Analysis Platform. *J. Cheminform.* **2012**, *4:17*.
26. Avogadro: An Open-Source Molecular Builder and Visualization Tool. Version 1.1.1. http://avogadro.openmolecules.net/.
27. Spek, A. L. Structure Validation in Chemical Crystallography. *Acta Crystallographica Section D* **2009**, *65*, 148-155.
28. Momma, K.; Izumi, F. VESTA: A Three-Dimensional Visualization System for Electronic and Structural Analysis. *J. Appl. Crystallogr.* **2008**, *41*, 653-658.
29. Phillips, J.; Braun, R.; Wang, W.; Gumbart, J.; Tajkhorshid, E.; Villa, E.; Chipot, C.; Skeel, R.; Kalé, L.; Schulten, K. Scalable Molecular Dynamics with NAMD. *J. Comput. Chem.* **2005**, *16*, 1781-1802.
30. Vanommeslaeghe, K.; Hatcher, E.; Acharya, C.; Kundu, S.; Zhong, S.; Shim, J.; Darian, E.; Guvench, O.; Lopes, P.; Vorobyov, I.; Mackerell, A. D. CHARMM General Force Field: A Force Field for Drug-Like Molecules Compatible with the CHARMM All-Atom Additive Biological Force Fields. *J. Comput. Chem.* **2010**, *31*, 671-690.
31. Björk, J.; Hanke, F.; Palma, C.; Samori, P.; Cecchini, M.; Persson, M. Adsorption of Aromatic and Anti-Aromatic Systems on Graphene through π−π Stacking. *J. Phys. Chem. Lett.* **2010**, *1*, 3407 - 3412.
32. Palma, C.; Ciesielski, A.; Oner, M. A.; Schaeffer, G.; Lehn, J.; Barth, J.; Samori, P. Two-Dimensional Soft Supramolecular Networks. *Chem. Commun.* **2015**, *51*, 17297 - 17300.
33. Winkler, A.; Hess, P. Study of the Energetics and Dynamics of Hydrogen Bond Formation in Aliphatic Carboxylic Acid Vapors by Resonant Photoacoustic Spectroscopy. *J. Am. Chem. Soc.* **1994**, *116*, 9233-9240.
34. Kampschulte, L.; Werblowsky, T. L.; Kishore, R. S. K.; Schmittel, M.; Heckl, W. M.; Lackinger, M. Thermodynamical Equilibrium of Binary Supramolecular Networks at the Liquid-Solid Interface. *J. Am. Chem. Soc.* **2008**, *130*, 8502-8507.
35. Tahara, K.; Okuhata, S.; Adisoejoso, J.; Lei, S.; Fujita, T.; De Feyter, S.; Tobe, Y. 2D Networks of Rhombic-Shaped Fused Dehydrobenzo[12]annulenes: Structural Variations under Concentration Control. *J. Am. Chem. Soc.* **2009**, *131 (48)*, 17583 - 17590.
36. Tahara, K.; Furukawa, S.; Uji-i, H.; Uchino, T.; Ichikawa, T.; Zhang, J.; Mamdouh, W.; Sonoda, M.; De Schryver, F. C.; De Feyter, S.; Tobe, Y. Two-Dimensional Porous Molecular Networks of Dehydrobenzo[12]annulene Derivatives via Alkyl Chain Interdigitation. *J. Am. Chem. Soc.* **2006**, *128*, 16613-16625.
37. Tao, F.; Bernasek, S. L. Complexity in the Self-Assembly of Bifunctional Molecules on HOPG: The Influence of Solvent Functionality on Self-Assembled Structures. *Langmuir* **2007**, *23*, 3513-3522.
38. Shao, X.; Luo, X.; Hu, X.; Wu, K. Solvent Effect on Self-Assembled Structures of 3,8-Bis-hexadecyloxy-benzo[c]cinnoline on Highly Oriented Pyrolytic Graphite. *J Phys Chem B* **2006**, *110*, 1288-1293.
39. Chen, X.; Luais, E.; Darwish, N.; Ciampi, S.; Thordarson, P.; Gooding, J. J. Studies on the Effect of Solvents on Self-Assembled Monolayers Formed from Organophosphonic Acids on Indium Tin Oxide. *Langmuir* **2012**, *28*, 9487-9495.
40. Valiyaveettil, S.; Enkelmann, V.; Moeßner, G.; Müllen, K. Approaches to Supramolecular Structures with Various Topologies in the Crystal Lattice. *Macromolecular Symposia* **1996**, *102*, 165-173.
41. Lavrich, D. J.; Wetterer, S. M.; Bernasek, S. L.; Scoles, G. Physisorption and Chemisorption of Alkanethiols and Alkyl Sulfides on Au(111). *J. Phys. Chem. B* **1998**, *102*, 3456-3465.
42. Barnard, R. A.; Matzger, A. J. Functional Group Effects on the Enthalpy of Adsorption for Self-Assembly at the Solution/Graphite Interface. *Langmuir* **2014**, *30*, 7388-7394.
43. Schwarz, D.; Noda1, Y.; Klouda, J.; Schwarzová-Pecková, K.; Tarábek, J.; Rybáček, J.; Janoušek, J.; Simon, F.; Opanasenko, M.V.; Čejka, J.; Acharjya, A.; Schmidt, J.; Selve, S.; Reiter-Scherer, V.; Severin, N.; Rabe, J.P.; Ecorchard, P.; He, J.; Polozij, M.; Nachtigall, P.; Bojdys, M.J. Twinned Growth of Metal-Free, Triazine-Based Photocatalyst Films as Mixed-Dimensional (2D/3D) van der Waals Heterostructures. *Adv. Mater.* **2017**, 1703399.

Table of Contents Graphic